

Comparative Analysis of Two Implant-Crown Connection Systems - A Finite Element Study

Rudi C. van Staden¹, Hong Guan¹, Yew-Chaye Loo¹, Newell W. Johnson², Neil Meredith³,

¹Griffith School of Engineering, Griffith University Gold Coast Campus, Australia;

²School of Dentistry and Oral Health, Griffith University Gold Coast Campus, Australia;

³Neoss Ltd, Harrogate, United Kingdom

The internal and external-hex connections of the Neoss and 3i implant systems, were compared in a three-dimensional Finite Element Analysis. Chewing forces of 200, 500 and 1000N and abutment screw preloads of 110, 320 and 550Nmm were studied. The connection type strongly influences the stress profile within the crown, with the external-hex connection exhibiting greater stresses than the internal-hex.

INTRODUCTION

Dental implants are a well accepted treatment for partially or totally edentulous subjects. Innovations through research have led to advancements in surgical and restorative techniques, improved surface features and restorative components. Dental implants typically use either internal-hex or external-hex connections with the crown (Figure 1 a). Although both connections are extensively used clinically, distinctly different stress distributions are produced within the crown. Clinicians have reported implant components linked to mechanical failure of crown and implant (Maeda et al. 2006, Merz et al. 2000, Khraisat et al. 2002). Two major factors may be implicated in crown and implant failure. These are;

- over tightening of the abutment screw leading to failure of the crown for internal-hex and external-hex connection type implant systems.
- excessive masticatory loads transferred from the occlusal plane of the crown to a stress concentration at the interface between the abutment and implant body.

Theoretical techniques such as the Finite Element Method (FEM) can be used to evaluate mechanical factors that could affect implant performance and success (Capodiferro et al. 2006, Gehrke et al. 2006, Huang et al. 2005, Khraisat et al. 2005). This study was undertaken using Finite Element Analysis (FEA) to aid understanding of the stresses in both internal-hex and external-hex implant systems under different loading conditions.

Studies by Maeda et al. (2006), Khraisat et al. (2002) and Merz et al. (2000) have all considered the stress within the abutment screw but disregarded the stress within the crown. To date no published research appears to have investigated the stress profile in the crown due to an internal-hex or external-hex connection. Ultimately, the outcome of this study will help dental practitioners to identify locations within the implant system susceptible to stress concentrations.

MATERIALS AND METHODS

The modelling and simulation herein are performed using the Strand7 FEA System (2004). The first step of the modelling is to define the geometry of the implant system. Then the material behaviour of the model is specified in terms of Young's modulus, Poisson's ratio and density for all components. The appropriate loading and restraint conditions are applied and the individual parameters and their contribution to the stress profile within the crown and implant is evaluated.

Modelling

Geometry for the implant systems were obtained from the manufacturers (Figure 1a). Section AA is set at a location where maximum compressive stresses occur within the crown, positioned at 30° from the x-axis towards the negative z-axis.

The parameters investigated are shown in Figure 1b. The implant is conical with 2 degrees of taper, a helical thread, outside diameter of 4.5mm and length of

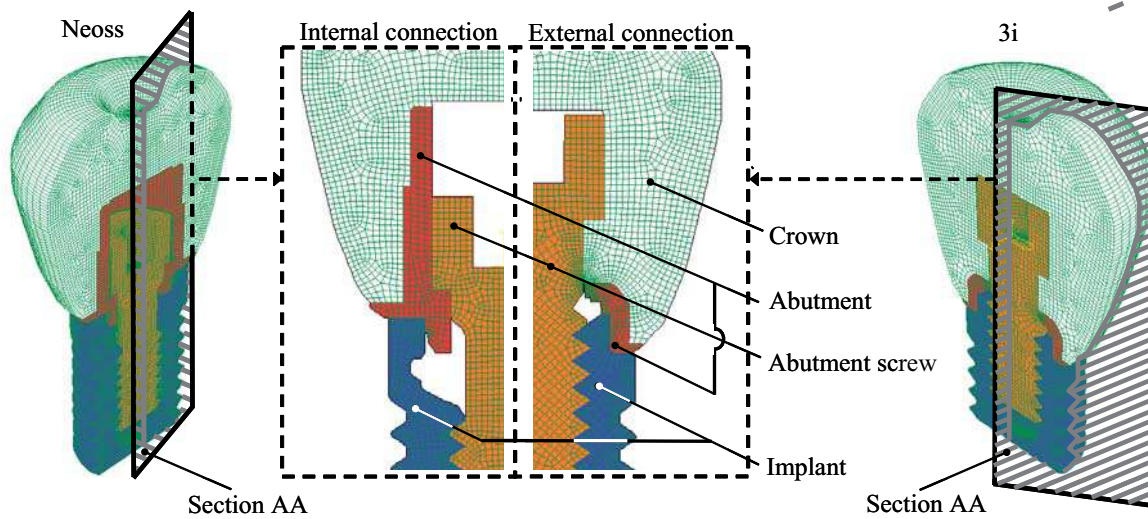
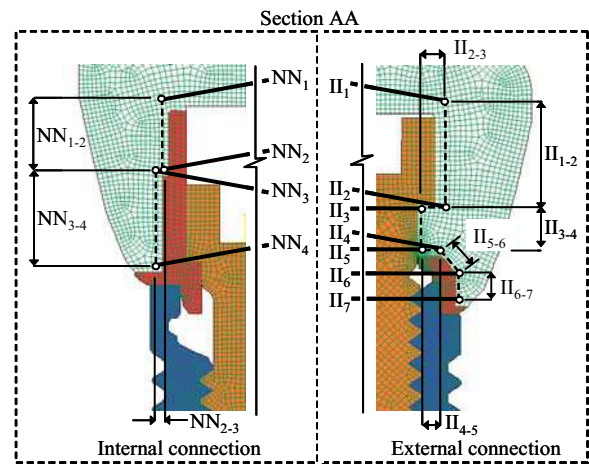
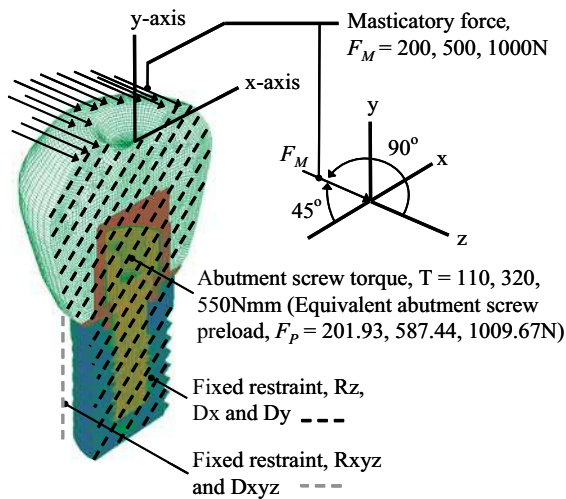


Fig. 1. Finite element model of external and internal-hex system

a) Implant system

b) Loading and restraint conditions (with detailed parameters)

c) Locations for measuring stress profile and contour



11 mm. Half the implant is modelled and symmetrical constraints are applied along the plane of symmetry as indicated (Figure 1b). For the Neoss (2006) and 3i (2006) finite element models, the total numbers of elements are respectively 13464 and 30420 for the implant, 3564 and 9108 for the abutment, 17424 and 25956 for the abutment screw, and 38484 and 47052 for the crown. The total number of nodal points for the entire Neoss model are 122688 and 82547 for the 3i.

The main focus of this study is to examine the stress characteristics within the crown and next to the crown-abutment interface. Therefore an assumption is made to restrain the outer edge of the implant (Figure 1b) when the mandibular bone is not included in the finite element model. Note that these loading and restraint conditions are the same for both internal and external-hex systems.

Stress reporting

The von Mises stresses along the lines NN (NN₁₋₂, NN₂₋₃ and NN₃₋₄) and II (II₁₋₂, II₂₋₃, II₃₋₄, II₄₋₅, II₅₋₆ and II₆₋₇) for both systems are reported for all possible combinations of loading (Figure 1 c). The relative locations of these lines are also detailed in the figure, which are identified by their start and end points. So, for example, the line II₁₋₂ begins at II₁ and ends at II₂. The von Mises stresses along the lines NN and II, in the crown, are believed to play a crucial role in the probability of crown fracture. On Section AA lines NN and II were chosen because the greatest stresses due to the masticatory loading (compressive is prominent over tensile) occur on this plane.

Material properties

The material properties in the model are specified in terms of Young's modulus, Poisson's ratio and density for the implant and all associated components (Table 1). All materials are assumed to exhibit linear, elastic and homogeneous behaviour.

Loading conditions

Masticatory force, F_M , was applied to the occlusal surface of the crown at 100, 250 or 500N, inclined at 45° to the x and y-axes (Figure 1 b). The preload, F_p , of 100.97, 293.72 or 504.84N is applied to the abutment screw through the use of temperature sensitive elements (Figure 1 b). Note that F_M and F_p are set to half of the total magnitude because only half of the implant system is modelled. Therefore the total F_M modelled is 200, 500, 1000N and F_p is 201.93, 587.44, 1009.67N. The manner of modelling the masticatory forces and the preload applied to the abutment screw was described by van Staden et al. (2008). For the purposes of this study both the abutment screw preload, F_p , and the surface area between abutment and abutment screw, SA_p , are halved when compared to those used by van Staden et al. (2008) due to the modelling assumption (half model). Calculations for the abutment screw surface pressure, q , confer identical results to those found by van Staden et al. (2008).

For the present study a negative temperature (-10 Kelvin, K) was applied to all the nodal points within the abutment screw, causing each element to shrink. A trial and error process was applied to determine the temperature coefficient, C , for the Neoss and 3i systems (i.e. C_{Neoss} and C_{3i}) that can yield an equivalent q . It was found that when $F_p = 201.93, 587.44$ and $1009.67N$ then $C_{Neoss} = -3.51 \times 10^{-4}, -9.28 \times 10^{-4}$ and $-15.60 \times 10^{-4} / K$, and $C_{3i} = -0.98 \times 10^{-4}, -1.80 \times 10^{-4}$ and $-2.68 \times 10^{-4} / K$, respectively.

RESULTS

Zirconia, typically used as a dielectric material, has proven adequate for application in dentistry. With its white appearance and high Young's modulus it is ideal for use in sub frames for dental restorations such as crowns and bridges, which can then be veneered with conventional feldspathic porcelain. Zirconia has a fracture strength greater than titanium; therefore it may be considered as a high strength material. However with masticatory and preload forces the compressive strength of 2.1 GPa (Curtis et al. (2005)) can easily be exceeded; especially for implant systems with external-hex connections, as confirmed during this study.

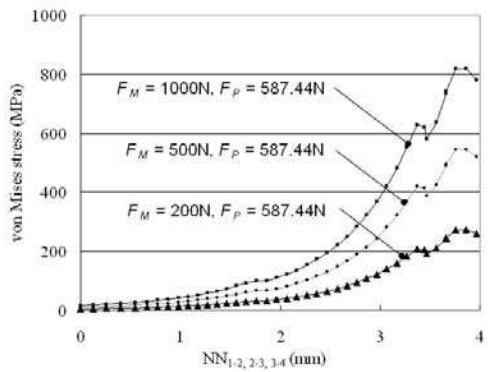
The distribution of von Mises stresses in the crown is discussed for all parametric combinations of masticatory and preload forces. Each parameter is discussed in a separate section. For the Neoss system, the von Mises stresses are reported between locations NN₁₋₂ (0-1.76mm in length), NN₂₋₃ (1.76-1.87mm) and NN₃₋₄ (1.87-3.96mm). For the 3i system the von Mises stresses are reported between locations II₁₋₂ (0-2.38mm), II₂₋₃ (2.38-2.78mm), II₃₋₄ (2.78-3.67mm), II₄₋₅ (3.67-4.06mm), II₅₋₆ (4.06-4.65mm) and II₆₋₇ (4.65-5.27mm), as shown in Figure 1c.

Masticatory Force, F_M

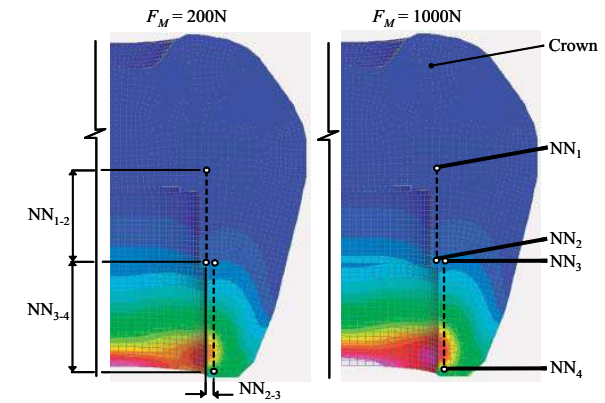
The distributions of von Mises stresses along the lines NN and II for all values of F_M are shown in Figure 2. Note that the preload, F_p , is set at its medium value, i.e. 587.44N.

Table 1. Material properties

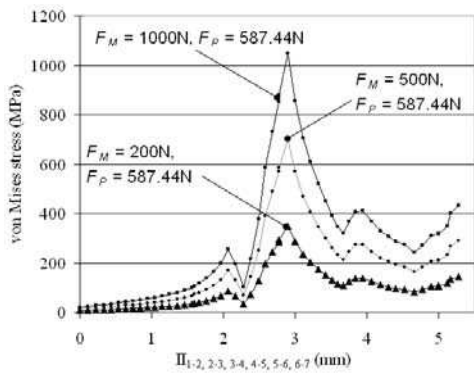
Component	Description	Young's Modulus, E (GPa)	Poissons ratio, v	Density, p (g/cm ³)
Implant, abutment, washer	Titanium (grade 4)	105.00	0.37	4.51
Abutment screw	Gold (precision alloy)	93.00	0.30	16.30



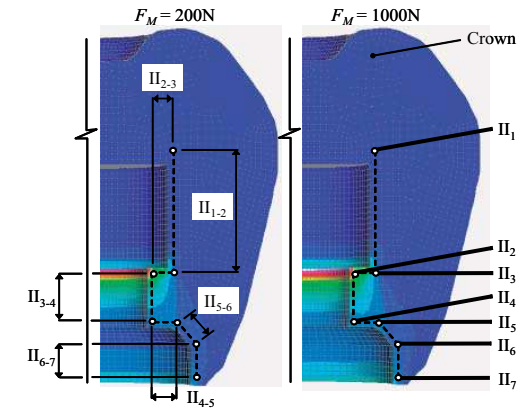
a) Stress profile



b) Stress contour



c) Stress profile



d) Stress contour

Figure 2. Stress characteristics when varying F_M

In general, when the applied masticatory force, F_M , is increased, the von Mises stresses also increase proportionally, because the system being analysed is linear elastic. When F_M increases the stress along the line NN increases showing two peaks along the line NN₃₋₄ (refer to Figure 2a). The larger of these two peaks occurs at a distance of ± 3.8 mm in length from NN₁. This stress peak (as can be identified in Figure 2 b) is caused by a sharp corner and sudden change in section at this point.

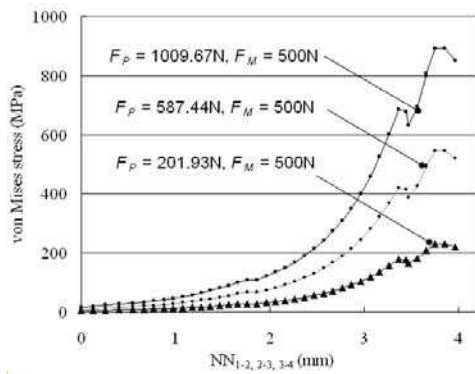
Elevated stress concentrations are identified at the beginning of the line II₃₋₄ (Figures 2 c and d). This stress peak, as can be identified in Figure 2 c, is caused by a sharp corner at this point. For the 3i system the volume of the crown exceeds that of the Neoss system, thereby suggesting that the 3i crown may show greater resistance to the applied masticatory forces. However, even though the Neoss crown has a thinner wall along the line NN₃₋₄, reduced stresses are still evident due to the

abutment's high Young's modulus. Overall, the design differences between the Neoss and 3i systems result in higher stresses in the 3i system when F_M is increased.

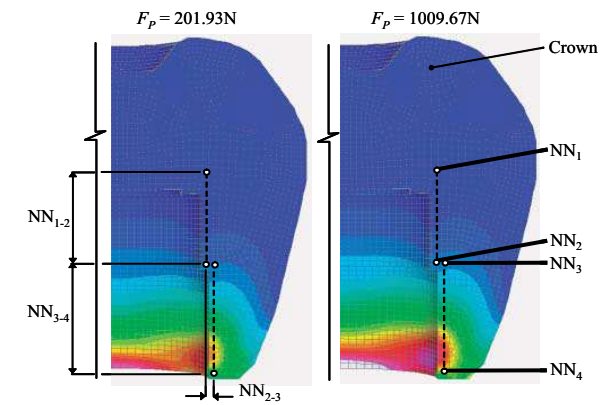
Preload Force, F_p

To investigate the effect of different preload F_p , F_M is kept as a constant and its medium value, i.e. 500N is considered herein. The distributions of von Mises stresses along the lines NN and II for all values of F_p are shown in Figure 3.

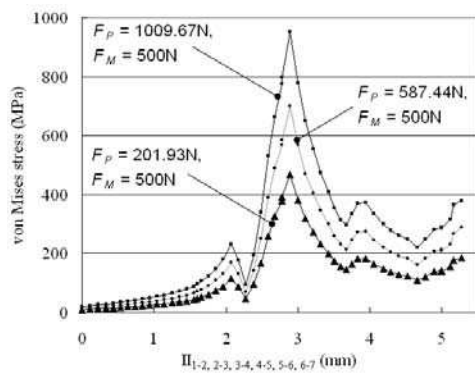
As found in Section 3.1 for F_M , when F_p increases the stresses calculated along the line NN increase, showing two peaks along the line NN₃₋₄ (refer to Figures 3 a and b). Also, as found for F_M , elevated stress peaks are identified at the beginning of the line II₃₋₄ (Figures 3 c and d). Overall, all values of F_M cause greater stresses along lines NN and II, than do varying values of F_p .



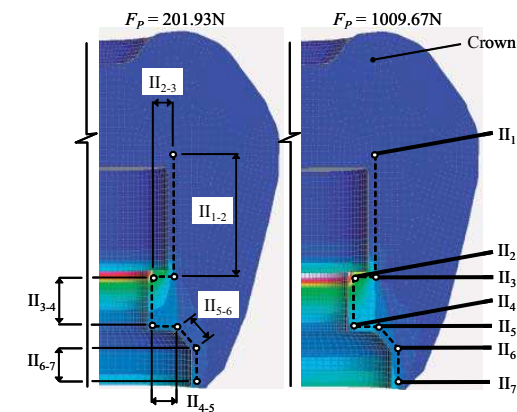
a) Stress profile



b) Stress contour



c) Stress profile



d) Stress contour

Figure 3. Stress characteristics when varying F_p

DISCUSSION

FEA has been used extensively to predict the biomechanical performance of the jawbone surrounding a dental implant (DeTolla et al. 2000, Geng et al. 2001). Previous research considered the influence of the implant dimensions and the bone-implant bond on the stress in the surrounding bone. However, to date no research has been conducted to evaluate the stress produced by different implant to crown connections (ie. internal-hex and external-hex).

The analysis completed in this paper uses the FEM to replicate internal-hex and external-hex connections for loading parameters of F_M and F_P . As shown in

Table 2, two stress peaks were revealed along the lines NN and II at locations 3.76 and 2.89mm from the top. The stress values shown were calculated with the other parameter (i.e. F_M or F_P) set to its average. The mastication force F_M is applied on the occlusal surface of the crown, evenly distributed along 378 nodal locations (Figure 1 b), and orientated at 45° in the x-y plane. This induces compressive stresses in the right hand side of the crown and tensile in the left. Varying F_M from 200 to 1000N for the internal-hex and external-hex systems results in a change in von Mises stress of 545.64 (818.47-272.82MPa) and 698.09MPa (1047.14-349.05MPa) respectively. The geometrical design of the external-hex system tends to induce stress concentrations, located 2.89mm

Table 2. von Mises stress (MPa) in the crown (location of stress reporting in brackets)

Parameter	----- F_M (N)-----			----- F_P (N)-----		
	200	500	1000	201.93	587.44	1009.67
Line						
NN (3.76mm)	272.82	545.64	818.47	231.55	545.64	891.83
II (2.89mm)	349.05	698.09	1047.14	466.21	698.09	951.67

from the apex in this study. For this system, a stress concentration at this point is also induced by F_p , increasing the compressive stresses on the right hand side of the crown. Increasing F_p from its minimum to maximum values, for the external-hex system, increases the stress by 485.46MPa (951.67-466.21MPa).

The internal-hex system has reduced stress concentrations, demonstrating that this design is less susceptible to stress concentrations within the crown. However, because of the transfer of the preload through the abutment screw to abutment contact, changing F_p is more influential on this hex system than F_M . Overall F_M is more influential on the stress within the crown for the external-hex system and F_p is more influential on the internal-hex system.

CONCLUSION

This research is a pilot study aimed at offering an initial understanding of the stress distribution characteristics in the crown under different loading conditions. Realistic geometries, material properties, loading and support conditions for the implant system were used.

The geometrical design of the external-hex system tends to induce stress concentrations in the crown at a distance of 2.89mm from the apex. At this location F_p also affects the stresses, so that the compressive stresses on the right hand side of the crown are increased. The internal-hex system has reduced stress concentrations in the crown. However, because the preload is transferred through the abutment screw to the abutment contact, changing F_p has greater effect on this hex system than F_M . Overall F_M is more influential on the stress within the crown for the external-hex system and F_p is more influential on the internal-hex system.

Future recommendations include the evaluation of other implant parameters such as the implant wall thickness and thread design. Ultimately, all implant components can be understood in terms of their influence on the stress produced within the implant itself.

ACKNOWLEDGEMENTS

This work was made possible by the collaborative support from Griffith's School of Engineering and School of Dentistry and Oral Health. A special thank you goes to Messires John Divitini and Ian Kitchingham from Neoss Limited for their continual contribution.

REFERENCES

- Capodiferro S, Favia G, Scivetti M, De Frenza G, Grassi R. Clinical management and microscopic characterisation of fatigue-induced failure of a dental implant. Case report. *Head and Face Medicine*. 2006;22(2):18.
- Curtis AR, Wright AJ, Fleming GJ. The influence of simulated masticatory loading regimes on the bi-axial flexure strength and reliability of a Y-TZP dental ceramic. *Journal of Dentistry*. 2006;34(5):317-325.
- DeTolla DH, Andreana S, Patra A, Buhite R, Comella B. Role of the finite element model in dental implants. *Journal of Oral Implantology*. 2000;26(2):77-81.
- Gehrke P, Dhom G, Brunner J, Wolf D, Degidi M, Piattelli A. Zirconium implant abutments: fracture strength and influence of cyclic loading on retaining-screw loosening. *Quintessence International*. 2006;37(1):19-26.
- Geng JP, Tan KB, Liu GR. Application of finite element analysis in implant dentistry: a review of the literature. *Journal of Prosthetic Dentistry*. 2001;85(6):585-598.
- <http://www.3i-online.com.htm> (accessed 12th July 2006).
- Huang HM, Tsai CM, Chang CC, Lin CT, Lee SY. Evaluation of loading conditions on fatigue-failed implants by fracture surface analysis. *International Journal of Oral & Maxillofacial Implants*. 2005;20(6):854-859.
- Khraisat A, Stegaroiu R, Nomura S, Miyakawa O. Fatigue resistance of two implant/abutment joint designs. *Journal of Prosthetic Dentistry*. 2002;88:604-610.
- Khraisat A. Stability of implant-abutment interface with a hexagon-mediated butt joint: failure mode and bending resistance. *Clinical Implant Dentistry Related Research*. 2005;7(4):221-228.
- Maeda Y, Satoh T, Sogo M. In vitro differences of stress concentrations for internal and external hex implant-abutment connections: a short communication. *Journal of Oral Rehabilitation*. 2006;33:75-78.
- Merz BR, Hunenbart S, Belser UC. Mechanics of the implant-abutment connection: an 8-degree taper compared to a butt joint connection. *International Journal of Oral & Maxillofacial Implants*. 2000;15:519-526.
- Neoss Limited (2006) Neoss Implant System Surgical Guidelines, UK.
- Strand7 Pty Ltd (2004) Strand7 Theoretical Manual, Sydney, Australia.
- van Staden RC, Guan H, Loo YC, Johnson NW, Meredith N. Stress Evaluation of Dental Implant Wall Thickness using Numerical Techniques. *Applied Osseointegration Research*. 2008 (In Press).